Title

Shubnikov–de Haas oscillations in electrodeposited single-crystal bismuth films

Journal

Physical Review B, 61(10)

ISSN

2469-9950

Authors

Yang, FY
Liu, Kai
Hong, Kimin
et al.

Publication Date

2000-03-01

DOI

10.1103/physrevb.61.6631

Peer reviewed

Shubnikov–de Haas oscillations in electrodeposited single-crystal bismuth films

F. Y. Yang, Kai Liu, Kimin Hong, and D. H. Reich
Department of Physics and Astronomy, The Johns Hopkins University, Baltimore, Maryland 21218

P. C. Searson
Department of Materials Science and Engineering, The Johns Hopkins University, Baltimore, Maryland 21218

C. L. Chien
Department of Physics and Astronomy, The Johns Hopkins University, Baltimore, Maryland 21218

Y. Leprince-Wang and Kui Yu-Zhang
Département de Physique, Université de Marne La Vallée, 5 Boulevard du Descartes/Champs sur Marne, 77454 Marne La Vallée Cedex 2, France

Ke Han
Center for Materials Science, Los Alamos National Laboratory, Los Alamos, New Mexico 87545
(Received 25 May 1999)

Shubnikov–de Haas oscillations have been observed in Bi thin films fabricated by electrodeposition. The observed dominant oscillation periods of 0.17, 0.08, and 0.077 T^{-1}, with the magnetic field along the trigonal, binary, and bisectrix axes of Bi, respectively, are in good agreement with those in bulk Bi single crystals.

I. INTRODUCTION

Bismuth (Bi), a semimetallic element, has many unusual electronic properties due to its highly anisotropic Fermi surface, low carrier concentrations, small carrier effective masses, and very long carrier mean free paths. In single crystals, these characteristics lead to very large magnetoresistance (MR) effects[1,2] and pronounced quantum oscillations. Among the latter are Shubnikov–de Haas (SdH) oscillations in the magnetoresistance and the de Haas–van Alphen oscillations in the susceptibility. Because of its long mean free path, and long Fermi wavelength, Bi is an attractive medium for the exploration of finite-size effects and quantum transport phenomena. For these studies, materials with lower dimensions such as thin films and nanowires are often required.[3–5] Unfortunately, most deposition methods yield Bi films that are polycrystalline with small grains,[6–8] which are undesirable for these purposes. It is possible, however, to grow epitaxial Bi films on BaF_2 substrates by molecular-beam epitaxy (MBE).[5,8,9] These MBE-grown thin films represent the best quality Bi films available up to now.

Recently we have successfully fabricated both Bi nanowires[10,11] and single-crystal thin films[12,13] by electrodeposition. The films exhibit very large MR effects, showing as much as a 3800-fold (or 380 000%) increase in the resistance at low temperatures and a 2.5-fold (250%) increase at room temperature with a nonhysteretic and quasilinear field dependence. These MR effects are certainly a useful measure of the quality of the Bi films, but the observation of quantum oscillations such as the SdH effect provides a more stringent test. Because the Fermi surface of Bi is highly anisotropic, as shown in Fig. 1, the SdH oscillations exhibit very different characteristics and periods when the magnetic field is applied along different symmetry axes. In this work, we report the observation of clean, anisotropic SdH oscillations for magnetic fields applied along the trigonal, bisectrix, and binary axes in electrodeposited Bi thin films. The oscillation periods are in good agreement with those previously determined from bulk single crystals.[14] These results show that the crystalline coherence of these films is maintained over macroscopic distances (e.g., cm), and provide further evidence that electrodeposition is a low-

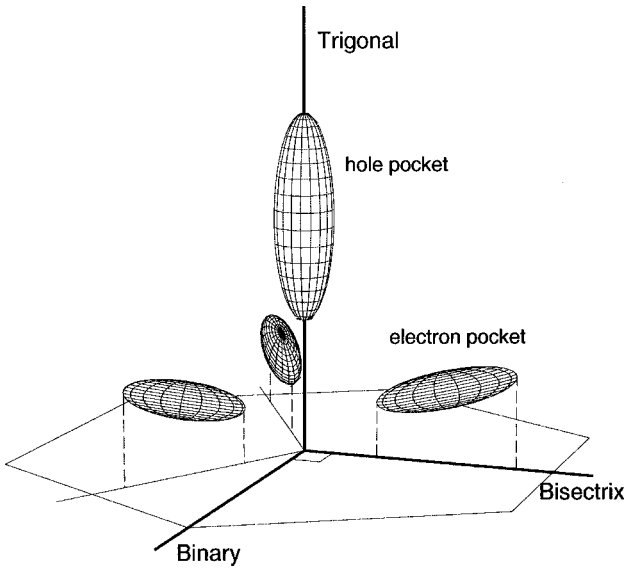

FIG. 1. Schematic of the Fermi surface of Bi showing the hole pocket along the trigonal axis and the three electron pockets in a plane perpendicular to the trigonal axis. The electron pockets are 120° apart in the plane that contains the bisectrix and the binary axes with a 6° tilt out of plane.

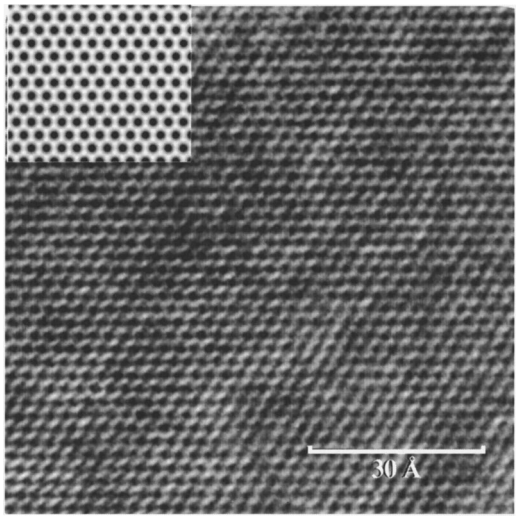

FIG. 2. High-resolution TEM image of a single-crystal Bi film showing the hexagonal atomic arrangement of the *c* plane. The inset shows a simulated lattice image of the plane.

cost, high-rate alternative to molecular-beam epitaxy techniques for the production of high-quality Bi thin films.

II. FABRICATION AND CHARACTERIZATION

The Bi films were electrodeposited from aqueous solutions of $Bi(NO_3)_3 \cdot 5H_2O$ onto a thin Au underlayer ($\sim$100-Å thick) patterned on a Si (100) wafer. The as-deposited Bi films, which we have grown up to 20-μm thick, are polycrystalline, but with large grains whose sizes are comparable to the film thickness. After annealing at 268°C in Ar for approximately 6 h, they become single crystalline. The details of the fabrication and processing have been described elsewhere.[10,12] Bismuth has a rhombohedral crystal structure, which is usually described in a hexagonal system with the trigonal axis as the *c* axis as shown in Fig. 1. The samples used in this work are trigonal-axis (001) single-crystal Bi films 10-μm thick. The details of x-ray-diffraction results have been published elsewhere.[12,13] High-resolution transmission electron microscopy (TEM) has also been used to characterize the Bi films. A plan view of the *c* plane of a single-crystal film is shown in Fig. 2, showing the sixfold symmetry of the atomic arrangement in this plane. The TEM image is also in agreement with a simulated TEM image for Bi, as shown in the inset of Fig. 2.

III. MAGNETORESISTANCE MEASUREMENTS

The basic magnetotransport properties of the Bi films, including the thickness and temperature dependence of the resistivity and the field dependence of the MR for temperatures $T>5$ K have been published elsewhere.[12,13] In this work, we focus on the SdH oscillations at low temperatures, measured in a 10-μm-thick single-crystal Bi film. MR measurements were carried out in a He^3-He^4 dilution refrigerator at temperatures between 0.06 and 10 K in magnetic fields *H* up to 9 T. X-ray pole figure measurements were used to determine the orientation of the crystal axes of the film, and a 6 $\times$2-mm sample was cut with its long axis parallel to the Bi bisectrix axis. A conventional ac four-probe method with the

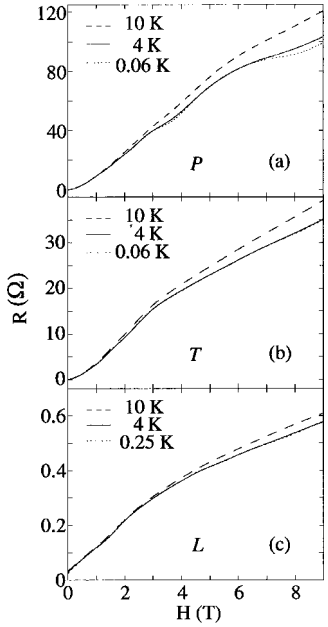

FIG. 3. Magnetoresistance of a 10-μm-thick single-crystal Bi film in the (a) perpendicular *P*, (b) transverse *T*, (c) longitudinal *L* geometry at various temperatures.

current along the long dimension of the sample was used to measure the resistance. The Fermi surface of Bi consists of three equivalent ellipsoidal electron pockets and one ellipsoidal hole pocket as shown in Fig. 1. The hole ellipsoid is symmetric about the trigonal axis with its long axis along the trigonal axis. The three electron ellipsoids are located symmetrically about the trigonal axis and lie essentially in a plane perpendicular to the trigonal axis. The bisectrix axis is below the center of one electron ellipsoid and perpendicular to the trigonal axis, and the binary axis is perpendicular to both the trigonal and the bisectrix axes. The long axis of that electron ellipsoid is in the bisectrix-trigonal plane with a tilt angle of about 6° from the bisectrix axis. The other two electron ellipsoids can be obtained through rotations of $\pm 120°$ about the trigonal axis.

In our experiment, the measuring geometries were as follows:

perpendicular (P): $\mathbf{H}\perp$ film, $\mathbf{H}\perp$ current, and $\mathbf{H}\parallel$ trigonal axis;

transverse (T): $\mathbf{H}\parallel$ film, $\mathbf{H}\perp$ current, and $\mathbf{H}\parallel$ binary axis;

longitudinal (L):

$\mathbf{H}\parallel$ film, $\mathbf{H}\parallel$ current, and $\mathbf{H}\parallel$ bisectrix axis.

The measured MR for the three geometries is shown for selected temperatures in Fig. 3. For this 10-μm film, the MR ratio, defined as $[R(H)-R(0)]/R(0)$, is about 1500 at 5 K and 5 T.[12] Even larger MR ratios have been observed in thicker Bi films.[13] While the MR is temperature dependent at higher temperature, both the carrier mean free path (limited by the film thickness) and the zero-field resistivity are essentially constant at very low temperatures. Thus the MR, aside from the SdH oscillations, does not vary appreciably below about 4 K for all three geometries, as can be seen from Fig. 3. Another prominent feature is that the overall size of the MR is the largest in the *P* geometry, smallest in the *L* geom-

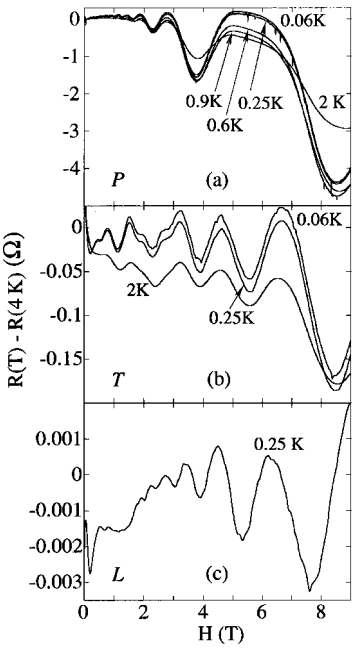

FIG. 4. Shubnikov–de Haas oscillations, displayed as $R(\mathrm{T})-R(4\ \mathrm{K})$, versus magnetic field H in (a) the perpendicular P geometry at $T=0.06$, 0.25, 0.6, 0.9, and 2 K, (b) the transverse T geometry at $T=0.06$, 0.25, and 2 K, and (c) the longitudinal L geometry at $T=0.25$ K.

etry, and intermediate for the T geometry. This is due to the different orientation of the cyclotron orbits with respect to the film in the three geometries.[12]

IV. SDH OSCILLATIONS IN MR

It is clear from Fig. 3 that there is additional structure in the MR curves and that the amplitude of this structure becomes larger at lower temperatures and at higher magnetic fields. These are the SdH oscillations. Utilizing the aforementioned insensitivity of the overall MR to temperature below 4 K, we can show the SdH oscillations more prominently by subtracting the data at 4 K from those at lower temperatures. This is shown in Fig. 4 for the three measuring geometries (P,T, and L) at different temperatures. First, we note that the oscillation amplitude is temperature dependent, increasing strongly with decreasing temperatures, before apparently saturating at the lowest temperatures. Second, the oscillation amplitude is geometry dependent, being the largest for the P geometry and the smallest for the L geometry. This is a reflection of the orientation-dependence of the magnitude of the MR as mentioned above. Third, the oscillation periods in the P,T, and L geometry are very different. This is due to the different extremal cross sections of the Bi Fermi surface when the magnetic field is applied along the trigonal, bisectrix, and binary axes as described below.

The SdH oscillations are due to the Landau quantization of the cyclotron orbits of the carriers.[15] In an external magnetic field **H** applied along the z direction, the electron and hole orbits are quantized into Landau levels with energies of

$$E=\left(\nu+\frac{1}{2}\right)\hbar\omega_c+\hbar^2k_z^2/2m^*, \tag{1}$$

where m^* is the carrier effective mass, $\omega_c=eH/m^*c$ is the cyclotron frequency, ν is an integer, and $\hbar k_z$ is the component of the momentum parallel to **H**. With increasing field, the occupancy of each Landau level and the separation between adjacent Landau levels, $\hbar\omega_c$, become larger. As a result, the Landau levels below the Fermi level are sequentially driven across the Fermi level. Accompanying the crossing of the Landau levels are abrupt changes of the density of states, which give rise to oscillations in the resistivity. As we indeed observe, the SdH oscillations are most prominent at low temperatures where the Landau levels are sharply defined. At higher temperatures, when $k_BT\gg\hbar\omega_c=\hbar eH/m^*c$, the oscillations are masked by thermal excitations between the Landau levels. The temperature dependence of the amplitude of SdH oscillations is approximately $\exp(-k_BT/\hbar\omega_c)$, further reduced by a factor of $\exp(-1/\omega_c\tau)$ due to impurity scattering.[15] Thus the amplitude of SdH oscillations does not vary appreciably below the Dingle temperature $T_D=\hbar/k_B\tau$, where $\tau=l/v_F=lm^*/\hbar k_F$ is the carrier relaxation time. In our 10-μm Bi film, $k_F\sim 2\times10^8\ \mathrm{m}^{-1}$ and l has been determined to be 7 μm,[12,13] giving $T_D\approx 0.4$ K. This is consistent with the lack of temperature dependence we observed in the SdH amplitude below $T=0.25$ K. The positions of the oscillations in each geometry, however, do not vary with temperature.

V. SDH OSCILLATION PERIOD

The SdH oscillations are periodic in $1/H$, with a period of

$$\Delta(1/H)=2\pi e/\hbar cA, \tag{2}$$

which is inversely proportional to the extremal cross-sectional area A of the Fermi surface in the plane normal to **H**. In determining the period, by convention, the minima in the MR curve are considered as the locations of the SdH oscillations. Figures 5(a)–5(c) shows the oscillations in $R(T)-R(4K)$, versus $1/H$ at 0.06, 0.06, and 0.25 K for the P,T, and L geometries, respectively. To display the oscillations at small fields more clearly, we have enlarged the scale of the small-field part of the oscillations by 30 and 4 times for the P and T geometries, respectively. The peak positions of the SdH oscillations in all three geometries are listed in Table I.

To facilitate the discussion, the extremal cross sections of the Fermi surface in all three geometries are shown next to the corresponding data [Figs. 5(d)–5(f)]. In the following, we will use the subscripts P,T, and L to represent the geometry, and h and e to mark the contribution from the hole or electron Fermi ellipsoids. For example, $A_{P,h}$ and $\Delta(1/H)_{P,h}$ are, respectively, the extremal cross section and the SdH oscillation period of the hole band in the perpendicular geometry.

In the perpendicular geometry, with **H** parallel to the trigonal axis, all three electron ellipsoids are equivalent, as shown in Fig. 5(d). There are only two extremal cross sections $A_{P,h}$ and $A_{p,e}$, hence there can be at most two periods of $\Delta(1/H)_{P,h}$ and $\Delta(1/H)_{P,e}$. However, for fortuitous reasons, the cyclotron masses ($0.065m_0$ for electrons and $0.064m_0$ for holes) and the extremal cross section of the hole ellipsoid and the electron ellipsoids are nearly the same.[14] Thus there is effectively only one period as observed. It

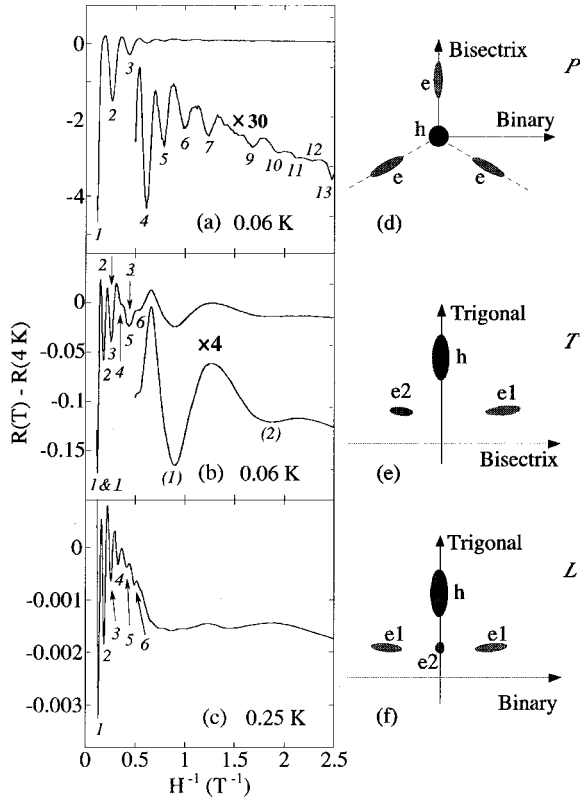

FIG. 5. Shubnikov–de Haas oscillations versus inverse magnetic field $1/H$ in (a) perpendicular P and (b) transverse T geometries at $T=0.06$ K and (c) longitudinal L geometry at $T=0.25$ K with the order n indicated. In (b), numbers from 1 to 6 are from the hole h band, and numbers with underlines and parenthesis are from electron bands $e1$ and $e2$, respectively. Portions of the results in (a) and (b) for $H^{-1}>0.5$ T^{-1} have been enlarged by 30 and 4 times, respectively. The extremal cross sections of the Fermi surface perpendicular to H are shown in the (d) perpendicular, (e) transverse, and (f) longitudinal geometries.

should be noted that because the mobility of the electrons is about a factor of 10 larger than that of the holes,[9] most of the contribution to the SdH oscillations comes from the electrons. The locations of the SdH minima and their corresponding order n from 1 to 13 are labeled in Figs. 5(a) and 6. The oscillation at $n=8$ was obscured by scale change of the

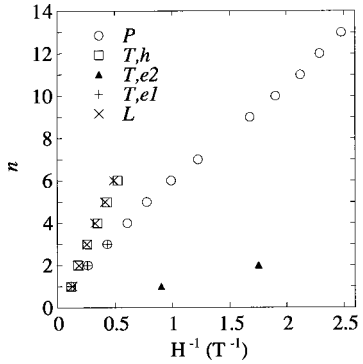

FIG. 6. The order n of the Shubnikov–de Haas oscillations in perpendicular P, transverse T, and longitudinal L geometries of a 10-μm-thick Bi film vs inverse magnetic field $1/H$. $h,e1$, and $e2$ refer to the hole and electron bands as described in the text.

instruments during the measurements. It may be noted that, as it is common, the number n is used to identify the SdH peaks and not the Landau levels. As shown in Fig. 6, the order n depends essentially linearly on inverse magnetic field but with a slight curvature, due to the movement of the Fermi level at high magnetic fields.[14] Using the low-field portion ($H^{-1}>1.6$ T^{-1}) of the oscillations ($n\geqslant 9$), we have determined that the periods for the holes and electrons in the perpendicular geometry to be

$$\Delta(1/H)_{P,h}\approx\Delta(1/H)_{P,e}\approx 0.20\ \mathrm{T}^{-1}, \tag{3}$$

which is slightly larger than the value of 0.16 T^{-1} reported for bulk single-crystal Bi.[16] This deviation is most likely due to a small misalignment of the sample with respect to the magnetic field. From the high field portion ($H^{-1}<1.1$ T^{-1}) of the oscillations ($n<7$), the periods for both carriers are 0.17 T^{-1}.

In the transverse geometry (T), with **H** parallel to the binary axis, as shown in Fig. 5(e), there are three different extremal cross sections: $A_{T,h}$ from the holes, and $A_{T,e1}$ and $A_{T,e2}$ from the electrons. Their areas are in the order $A_{T,h}>A_{T,e1}>A_{T,e2}$, and hence the order of the periods is $\Delta(1/H)_{T,h}<\Delta(1/H)_{T,e1}<\Delta(1/H)_{T,e2}$. The hole ellipsoid has the shortest period and the electron ellipsoids with the smaller $A_{T,e2}$ have the largest period. Because $A_{T,e1}$ in the T geometry is nearly the same as $A_{P,e}$ in the P geometry, as shown in Figs. 5(d) and (e), one expects

$$\Delta(1/H)_{T,e1}\approx\Delta(1/H)_{P}\approx 0.17\ \ \mathrm{T}^{-1} \tag{4}$$

in high field ($H^{-1}<1.1$ T^{-1}). However, an inspection of Fig. 4 reveals that the dominant period in the T geometry is not that described by Eq. (4), but roughly half of that. This shorter period can only be that due to the hole ellipsoid. As shown in Fig. 5(b), six minima with $H^{-1}<0.55$ T^{-1} are equally spaced, corresponding to a period of

$$\Delta(1/H)_{T,h}\approx 0.08\ \ \mathrm{T}^{-1}. \tag{5}$$

Because the two periods (0.17 and 0.08 T^{-1}) shown in Eqs. (4) and (5) differ by nearly a factor of 2, the SdH oscillations of the electron ellipsoid $A_{T,e1}$ with a larger cross section nearly coincide with every other SdH oscillations of the hole ellipsoid. Hence the $A_{T,e1}$ oscillations with underlined number $n=\underline{1},\underline{2},\underline{3}$ essentially coincide with those of $A_{T,h}$ with $n=1,3,5$. It is not $n=2,4,6$ because of the locations of the peaks from $1/H=0$.

For the SdH oscillations of the electron ellipsoid with the smaller cross section $A_{T,e2}$, it is known that its lowest Landau level will reach the Fermi level at a field less than 2 T,[17] and thus can only contribute to the SdH oscillations at $H^{-1}>0.5$ T^{-1}. In this region of H^{-1}, as shown in Fig. 5(b), there are two minima at $H^{-1}=0.91$ and 1.75 T^{-1}, labeled by (1) and (2), giving a period of

$$\Delta(1/H)_{T,e2}\approx 0.84\ \ \mathrm{T}^{-1}, \tag{6}$$

which is the same as that observed in bulk single crystals.

Finally, in the longitudinal geometry (L), with **H** parallel to the bisectrix axis, as shown on the right side of Fig. 5(c), there are three different extremal cross sections: one hole ellipsoid $A_{L,h}$, two electron ellipsoids of a larger size $A_{L,e1}$,

TABLE I. Shubnikov–de Haas Oscillation positions of Bi single-crystal thin films in H(T) and $1/H(\mathrm{T}^{-1})$, and the oscillation period $\Delta(1/H)$ in the perpendicular, transverse, and longitudinal geometries due to holes (h) and electrons (e).

Perpendicular			Transverse			Longitudinal		
H(T)	$1/H$	Origin(n)	H(T)	$1/H$	Origin(n)	H(T)	$1/H$	Origin(n)
8.62	0.116	$h,e(1)$	8.46	0.118	h(1)	7.62	0.131	h(1)
3.77	0.265	$h,e(2)$	5.57	0.180	h(2)	5.33	0.188	h(2)
2.30	0.435	$h,e(3)$	3.84	0.260	h(3)	3.89	0.257	h(3)
1.64	0.610	$h,e(4)$	2.87	0.348	h(4)	3.05	0.328	h(4)
1.29	0.775	$h,e(5)$	2.30	0.435	h(5)	2.40	0.417	h(5)
1.01	0.990	$h,e(6)$	1.91	0.524	h(6)	2.03	0.493	h(6)
0.82	1.22	$h,e(7)$						
			8.46	0.118	e1(1)			
0.60	1.67	$h,e(9)$	3.84	0.260	e1(2)			
0.53	1.89	$h,e(10)$	2.30	0.435	e1(3)			
0.48	2.07	$h,e(11)$						
0.44	2.26	$h,e(12)$	1.11	0.90	e2(1)			
0.41	2.45	$h,e(13)$	0.57	1.75	e2(2)			

and one electron ellipsoid of a smaller size $A_{L,e2}$. The three sizes are in the order $A_{L,h}>A_{L,e1}>A_{L,e2}$. The area $A_{L,h}$ should be nearly the same as $A_{T,h}$ in the T geometry, and hence should have a similar period. From the L geometry data, we have determined the period

$$\Delta(1/H)_{L,h}\approx 0.077\ \ \mathrm{T}^{-1}, \tag{7}$$

which is indeed very close to that of Eq. (5). Of the three electron ellipsoids, the electron ellipsoid with the smallest extremal cross section $A_{L,e2}$ does not appreciably contribute to the SdH oscillations because its lowest Landau level reaches the Fermi level at a very small magnetic field. The two ellipsoids with larger extremal cross section $A_{L,e1}$ also do not contribute in the high-field region ($H^{-1}<0.5\ \mathrm{T}^{-1}$). They at most indicate hints of the SdH oscillations in the low-field region of $H^{-1}>0.5\ \mathrm{T}^{-1}$ as shown n Fig. 5(c). Thus all the sharp SdH oscillations in the L geometry at $H^{-1}<0.5\ \mathrm{T}^{-1}$ are due to holes with a period shown in Eq. (7), with n up to 6.

In summary, we have observed clean SdH oscillations with the magnetic field along the trigonal, bisectrix, and binary axes in single-crystal Bi thin films fabricated by electrode position. The observed periods of the SdH oscillations are in good agreement with those obtained from bulk single crystals. The SdH oscillations in all three geometries are very different due to the highly anisotropic Fermi surfaces of bismuth. In each case, oscillations due to the portion of the Fermi surface with the largest extremal cross section dominate. In the perpendicular, transverse, and longitudinal geometries, the dominant oscillation periods are 0.17, 0.08, and 0.077 T^{-1}, respectively. These results demonstrate that the film used in this work is a large single crystal. If this were not so, and the sample contained as few as two misaligned grains, the SdH oscillations in the three different geometries would not show the expected dominant period. The SdH results reported here attest to the high quality of the electrodeposited single-crystal Bi films, and pave the way for further quantum transport studies.

ACKNOWLEDGMENTS

This work has been supported by NSF Grant Nos. DMR96-32526, DMR97-32763, and DMR93-57518.

[1] P.B. Alers and R.T. Webber, Phys. Rev. **91**, 1060 (1953).
[2] J.H. Mangez, J-P. Issi, and J. Heremans, Phys. Rev. B **14**, 4381 (1976).
[3] Yu.F. Komnik, E.I. Bukhshtab, Yu.V. Nikitin, and V.V. Andrievskii, Zh. Éksp. Teor. Fiz. **60**, 669 (1971) [Sov. Phys. JETP **33**, 364 (1971)].
[4] C.A. Hoffman, J.R. Meyer, F.J. Bartoli, A. Di Venere, X.J. Yi, C.L. Hou, H.C. Wang, J.B. Ketterson, and G.K. Wong, Phys. Rev. B **48**, 11 431 (1993).
[5] M. Lu, R.J. Zieve, J.A. van Hulst, H.M. Jaeger, T.F. Rosenbaum, and S. Radelaar, Phys. Rev. B **53**, 1609 (1996).
[6] D.E. Beutler and N. Giordano, Phys. Rev. B **38**, 8 (1988).
[7] T. Missana, C.N. Afonso, Appl. Phys. A: Mater. Sci. Process. **62**, 513 (1996).
[8] J.A. van Hulst, H.M. Jaeger, and S. Radelaar, Phys. Rev. B **52**, 5953 (1995).
[9] D.L. Partin, J. Heremans, D.T. Morelli, C.M. Thrush, C.H. Olk, and T.A. Perry, Phys. Rev. B **38**, 3818 (1988).
[10] K. Liu, C.L. Chien, P.C. Searson, and Kui Yu-Zhang, Appl. Phys. Lett. **73**, 1436 (1998).
[11] K. Liu, C.L. Chien, and P.C. Searson, Phys. Rev. B **58**, R14 681 (1998).
[12] F.Y. Yang, Kai Liu, C.L. Chien, and P.C. Searson, Phys. Rev. Lett. **82**, 3328 (1999).

[13] F.Y. Yang, Kai Liu, Kimin Hong, D.H. Reich, P.C. Searson, and C.L. Chien, Science **284**, 1335 (1999).
[14] G.E. Smith, G.A. Baraff, and J.M. Rowell, Phys. Rev. **135**, A1118 (1964).
[15] J. M. Ziman, *Principles of the Theory of Solids* (Cambridge University Press, New York, 1964).
[16] J.S. Dhillon and D. Shoenberg, Philos. Trans. R. Soc. London **248**, 1 (1955).
[17] K. Hiruma and N. Miura, J. Phys. Soc. Jpn. **52**, 2118 (1983).